Robotica (2017) volume 35, pp. 2139–2156. © Cambridge University Press 2016
doi:10.1017/S0263574716000758

Adaptive tracking control of multi-link robots actuated by pneumatic muscles with additive disturbances

Tarapong Karnjanaparichat and Radom Pongvuthithum*

Department of Mechanical Engineering, Faculty of Engineering, Chiang Mai University, Chiang Mai 50200, Thailand

(Accepted September 21, 2016. First published online: October 26, 2016)

SUMMARY

In this paper, we study the problem of adaptive position tracking for a multi-link robot driven by two opposing pneumatic muscle groups with additive disturbances. In contrast to widely used sliding mode control methods, the proposed controller is continuous and able to prevent chattering. All physical parameters of the robot and the pneumatic muscles, including pneumatic muscle coefficients, link lengths and moments of inertia are unknown and can be time-varying and the unknown additive disturbances can be discontinuous. Under these conditions, we prove that closed-loop trajectories of all of the joint positions can track any $\mathbf{C^1}$ joint reference signal. The joint errors will be within a prescribed error bound in a finite time. The adaptive controller only uses the reference signal, not its derivative. The continuous adaptive gain is one-dimensional. Simulations including a two-link robot arm with friction and realistic muscle models are presented to demonstrate the robustness of the adaptive control under severe changes of the system parameters. In all simulations, the joint positions can track $\mathbf{C^1}$ trajectories and all errors are within the prescribed error bound in the same time frame, even though the muscle parameters are vastly different.

KEYWORDS: Control of Robotic Systems; Robot Dynamics; Exoskeletons; Automation; Serial Manipulator Design and Kinematics.

1. Introduction

Actuators in conventional industrial robots are usually designed to have high stiffness to improve accuracy, stability and control bandwidth. For various new robotic applications such as wearable robots, rehabilitation robots, prosthetics and walking robots, accurate positioning or trajectory tracking is not the main objective. One of the main objectives of these applications is to have a light-weight and compliant actuator. Compliant actuators are utilized due to their abilities to absorb energy and safely interact with human.

Pneumatic muscles are a kind of compliant actuator that contracts when it is pressurized. There are many types of pneumatic muscles such as McKibben muscle or Braided muscle, Pleated muscle,[1] Yarlott Netted muscle,[2] ROMAC muscle[3] and Paynter Hyperboloid muscle.[4] Compared to other, more traditional actuators, these have many advantages including simple construction, light-weight, high power to weight ratio and intrinsic compliance. As a result, pneumatic muscles have been used in various applications such as bio-inspired, medical and industrial robots. Recent reviews of these applications can be found in Andrikopoulos *et al.*[5]

Mathematical models of pneumatic muscles can be divided into two main categories: static and dynamic. Static models were developed based on the principle of virtual work and the actual construction of braided muscles.[6–8] These models give the non-linear relations of contractile force, internal pressure and length of muscle. Later, Repperger *et al.*[9] proposed dynamic models in which a pneumatic muscle was treated as a spring element and a damping element arranged in parallel. Then, Reynolds *et al.*[10] proposed a three-element model such that a contractile element was added

* Corresponding author. E-mail: radom.p@cmu.ac.th

https://doi.org/10.1017/S0263574716000758 Published online by Cambridge University Press

in parallel to a spring element and a damping element. Due to their simple structures, these dynamic models have been widely used in many recent robot studies.[14–24]

Control of pneumatic muscles is difficult due to the muscle model non-linearity and its physical parameters also being non-linear and time-varying. Muscle properties can change with temperature and deterioration of the muscle materials can occur when the muscles are in use for an extended period of time. Researchers have proposed various control schemes for robots and mechanical systems actuated by pneumatic muscles. These control schemes range from a traditional PID control[29, 30] to neural network and fuzzy control,[31–34] iterative learning control (ILC) techniques,[35, 36] and a wildly used sliding mode control (SMC) and its variations.[11–22] PID control is simple to implement but only effective for a certain operating point and unable to adapt to parameter uncertainties or disturbances. To solve this problem, neural network and fuzzy controls are used to adapt PID gains. However, because of the complexity of the neural network and fuzzy logic structures, it is difficult to explicitly prove stability of the closed-loop system. In addition, these approaches also require training. From a theoretical stand point, SMC can ensure stability of systems and provide a good tracking performance in the presence of parametric uncertainty. However, SMC is discontinuous which may excite high-frequency unmodeled dynamics and cause chattering. Therefore, it cannot be directly applied. To prevent chattering, a saturation function is used instead of a signum function. This leads to various SMC laws such as boundary layer augmented SMC (BASMC)[14–17] and proxy-based SMC (PBSMC).[19, 20] Using a saturation function can prevent chattering but cannot guarantee asymptotic tracking. Only boundedness of system trajectories and the tracking error being within certain value can be achieved. Recently, Xu[26] proposed a chattering-free robust controller, which was later used for position control of a planar manipulator[21] and a gait training robot,[22] both actuated by pneumatic muscles. Unfortunately, Potluri[27] gave a counter example showing that Xu had overclaimed the results and chattering can occur. Xu also provided a response that concurred with Potluri's conclusions.[28]

When compared with using a fixed gain in robust control, an adaptive controller could provide a lower control gain since the gain will only be adapted to a necessary level. However, implementing an adaptive control for a robot can be difficult due to very high dimensions of the adaptive gain. In our previous work,[37] we showed that a continuous adaptive controller can solve a tracking problem for a single joint robot driven by pneumatic muscles without disturbance. In this paper, we extend the results from our previous work to a multi-link robot and prove that similar tracking performance can be achieved under systems with additive disturbances such as frictions and external forces. In addition, we propose a new continuous adaptive gain which improves the convergent rate of the error. The proposed controller is completely independent of all robot and muscle parameters and can adapt to system parameter changes and disturbances. The control law can guarantee that the closed-loop trajectories of all joint positions can track any continuously differentiable ($\mathbf{C^1}$) joint reference signal and the joint errors will be within a prescribed error bound in a finite time.

The proposed approach reduces the dimension of the adaptive gain to one. In addition, while other control designs require at least $\mathbf{C^2}$ reference trajectory, the proposed design only require that the reference trajectory is $\mathbf{C^1}$. This broadens the class of the reference trajectories that can be used. More importantly, the controller only uses the reference trajectory, not its derivative. This simplifies the process of converting the reference trajectory from the work space to the joint space since it eliminates the process of calculating the derivatives of the inverse Jacobian matrix.

The remainder of the paper is organized as follows. Section 2 introduces the pneumatic muscle model and some properties of the rigid robot, and formulates a dynamic model of a multi-link robot actuated by pneumatic muscles. The adaptive control scheme is presented in Section 3. Simulations for a two-link planar arm are presented in Section 4 to demonstrate the performance of the control law. Finally, conclusions are drawn in Section 5.

2. Dynamics of Multi-Link Robot Actuated by Pneumatic Muscles

2.1. Dynamics of pneumatic muscle actuator

In Reynolds *et al.,*[10] a pneumatic muscle is modeled using three elements: a spring, a damper and a contractile force, connected in parallel, as shown in Fig. 1. The total force exerted by the muscle is

$$R = F(P) - B(P)\dot{x} - K(P)x, \tag{1}$$

https://doi.org/10.1017/S0263574716000758 Published online by Cambridge University Press

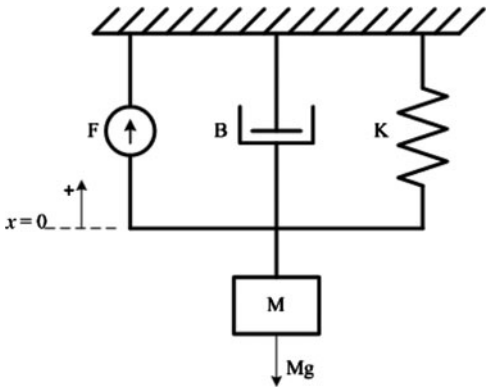


Fig. 1. A three-element model of the pneumatic muscle.

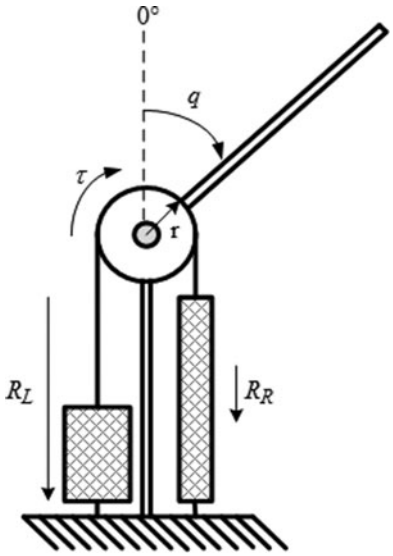


Fig. 2. The pneumatic muscle actuator configuration.

where P is internal pressure, F is the force exerted by the contractile element, B is the damping coefficient and K is the spring coefficient. Using data from experiments, the coefficients were formulated as polynomial functions of the muscle pressure.

The functions of the three elements are given by

$$K(P) = K_0 + K_1 P, \tag{2}$$

$$B(P) = B_0 + B_1 P \quad \text{(Inflation)}, \tag{3}$$

$$B(P) = B_0 - B_1 P \quad \text{(Deflation)}, \tag{4}$$

$$F(P) = F_0 + F_1 P\ . \tag{5}$$

In this paper, we consider a multi-link robot. Each joint of the robot is driven by a pneumatic muscle pair operating in antagonism similar to an actuator based on the physiological model of the bicep–tricep system shown in Fig. 2. The right and left muscle groups do not necessarily have the same muscle coefficients. The force differences between the two muscles generate a positive or negative torque.

Assuming that there are n muscle pairs tied together and attached to a sprocket of radius r, as in Fig. 2. The torque produced by the muscle pair is

$$\tau = \tau_R - \tau_L = n(R_R - R_L)r, \tag{6}$$

https://doi.org/10.1017/S0263574716000758 Published online by Cambridge University Press

where R_R and R_L are the total forces exerted by the right and left muscle groups, respectively. When the force $R_R > R_L$, the torque exerted on the joint is clockwise. From Eq. (1), we have

$$R_R = n(F_R - B_R\dot{x}_R - K_R x_R), \tag{7}$$

$$R_L = n(F_L - B_L\dot{x}_L - K_L x_L), \tag{8}$$

where x_R and x_L are the length of the right and left muscles. F_R, K_R and B_R depend on the internal pressure of the right muscles, whereas F_L, K_L and B_L depend on the internal pressure of the left muscles. Substituting Eqs. (7) and (8) into Eq. (6), the total torque delivered to the sprocket is

$$\tau = n(F_R - B_R\dot{x}_R - K_R x_R - F_L + B_L\dot{x}_L + K_L x_L)r. \tag{9}$$

Let the joint position $q = \pi(-\pi)$ rad. correspond to the left(right) muscles being fully extended. Therefore, the muscle lengths x_R and x_L can be expressed in terms of q as

$$x_R = (\pi + q)r, \tag{10}$$

$$x_L = (\pi - q)r. \tag{11}$$

Let the internal pressure of the right muscles, P_R, and left muscles, P_L, be

$$P_R = P_{0R} + \Delta p, \tag{12}$$

$$P_L = P_{0L} - \Delta p, \tag{13}$$

where P_{0R} and P_{0L} are nominal positive constant pressures, and Δp is a pressure input. With the definitions (12), (13), the antagonist pairs become a single-input system with input Δp.

From Eqs. (9)–(13) and the coefficient functions (2)–(5), the torque can be written as

$$\tau = -h(q, \dot{q}, b_A(\dot{q}))\Delta p - b_D(\dot{q})\dot{q} - a_E q - a_F, \tag{14}$$

where

$$h(\cdot) = b_A(\dot{q})\dot{q} + a_B q + a_C,$$

$$b_A(\dot{q}) = \begin{cases} -n(B_{1Li} + B_{1Rd})r^2, & \dot{q} < 0 \\ 0, & \dot{q} = 0 \\ n(B_{1Ld} + B_{1Ri})r^2, & \dot{q} > 0 \end{cases}$$

$$a_B = n(K_{1R} - K_{1L})r^2,$$

$$a_C = n(-F_{1R} - F_{1L} + rK_{1R}\pi + rK_{1L}\pi)r,$$

$$b_D(\dot{q}) = \begin{cases} n(B_{0Li} + B_{1Li}P_{0L} \\ +B_{0Rd} - B_{1Rd}P_{0R})r^2, & \dot{q} < 0 \\ 0, & \dot{q} = 0 \\ n(B_{0Ld} - B_{1Ld}P_{0L} \\ +B_{0Ri} + B_{1Ri}P_{0R})r^2, & \dot{q} > 0 \end{cases}$$

$$a_E = n(K_{1L}P_{0L} + K_{1R}P_{0R} + K_{0L} + K_{0R})r^2,$$

$$a_F = n(-F_{0R} - F_{1R}P_{0R} - rK_{1L}P_{0L}\pi + rK_{0R}\pi + F_{1L}P_{0L} + F_{0L} - rK_{0L}\pi + rK_{1R}P_{0R}\pi)r.$$

The subscripts, R and L, indicate the coefficients of right and left muscles, respectively. The subscripts, i and d, on the coefficient B denote whether the muscles are being inflated and deflated, respectively.

https://doi.org/10.1017/S0263574716000758 Published online by Cambridge University Press

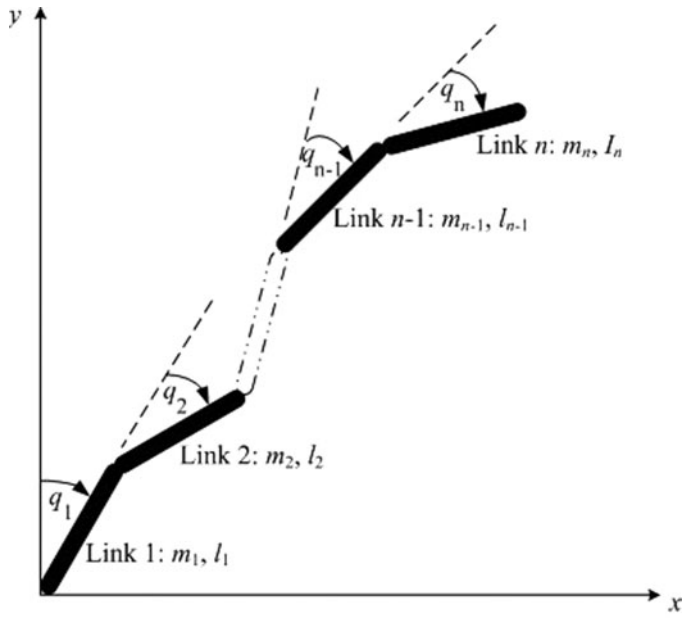


Fig. 3. Multi-link robot configuration.

2.2. Robot dynamics and some properties

The dynamics of a n-link rigid robot is given by Euler-Lagrange equation

$$D(q)\ddot{q} + C(q, \dot{q})\dot{q} + G(q) + \tau_d = \tau, \tag{15}$$

where $q \in \mathbb{R}^n$ is the relative joint position vector, $D(q)$ is the inertia matrix which is positive definite and symmetric, $C(q, \dot{q})\dot{q}$ is the coriolis and centrifugal term, $G(q)$ is the gravity vector, τ_d is an unknown disturbance including unknown payloads and friction forces and τ is the joint torque vector actuated by pneumatic muscles.

The rigid robot dynamics in Eq. (15) describe the behavior of robot manipulators, which are complex and highly non-linear. In what follows, we provide useful properties of a multi-link robot with revolute joints.

Property 2.1. The inertia matrix $D(q)$ is symmetric, positive definite and bounded. Thus,

$$\mu_m \leq \| D(q) \| \leq \mu_M,$$

where μ_m and μ_M are positive constants.

Property 2.2. There exists a constant $C_M \geq 0$ such that the matrix $C(q, \dot{q})$ is bounded by

$$\| C(q, \dot{q}) \| \leq C_M \| \dot{q} \| .$$

Property 2.3. $\dot{D}(q) - 2C(q, \dot{q})$ is skew-symmetric, i.e.

$$\xi^T \{\dot{D}(q) - 2C(q, \dot{q})\}\xi = 0 \qquad \forall \xi \in \mathbb{R}^n.$$

Property 2.4. The gravity vector is bounded by a constant $G_M \geq 0$, i.e.

$$\| G(q) \| \leq G_M.$$

https://doi.org/10.1017/S0263574716000758 Published online by Cambridge University Press

Assumption 2.1. The unknown disturbance is bounded by a constant $T_M \geq 0$, i.e.

$$\|\tau_d\| \leq T_M.$$

2.3. Dynamics of multi-link robots actuated by pneumatic muscles

In this section, we present general dynamical equations of a multi-link robot actuated by pneumatic muscles. From Eq. (14), the torque of the pneumatic muscle actuators driving the ith link is given by

$$\tau_i = -h_i(q_i, \dot{q}_i, b_{Ai}(\dot{q}_i))\Delta p_i - b_{Di}(\dot{q}_i)\dot{q}_i - a_{Ei}q_i - a_{Fi}, \tag{16}$$

where $h_i(\cdot)$ and $b_{Di}(\cdot)$ are unknown discontinuous functions, and a_{Ei} and a_{Fi} are unknown constants.

For a multi-link robot, it is common to write Eq. (16) in a matrix form:

$$\tau = -H(q, \dot{q}, b_{Ai}(\dot{q}_i))\Delta p - B_D(\dot{q})\dot{q} - A_E q - A_F, \tag{17}$$

where

$$\begin{aligned} \Delta p &= [\Delta p_1, \ldots, \Delta p_n]^T, \\ H(q, \dot{q}, b_{Ai}(\dot{q}_i)) &= diag\{h_1(\cdot), \ldots, h_n(\cdot)\}, \\ B_D(\dot{q}) &= diag\{b_{D1}(\dot{q}_1), \ldots, b_{Dn}(\dot{q}_n)\}, \\ A_E &= diag\{a_{E1}, \ldots, a_{En}\}, \\ A_F &= [a_{F1}, \ldots, a_{Fn}]^T. \end{aligned}$$

Finally, combining the rigid robot dynamics in Eqs. (15) and (16) yields the following model of a multi-link robot actuated by pneumatic muscles,

$$D(q)\ddot{q} + C(q, \dot{q})\dot{q} + G(q) + \tau_d = -H(q, \dot{q}, b_{Ai}(\dot{q}_i))\Delta p - B_D(\dot{q})\dot{q} - A_E q - A_F. \tag{18}$$

3. Adaptive Position Tracking Control

3.1. Problem statement

The problem of *adaptive position tracking* is formulated as follows. Given a constant $\epsilon > 0$ and a reference signal $q_r = [q_{1r}, \ldots, q_{nr}]^T \in \mathbf{C^1}$, find, if possible, an adaptive controller of the form:

$$\begin{aligned} \dot{\kappa} &= \alpha(q, q_r(t)), \quad \kappa \in \mathbf{R} \\ \Delta p &= \mu(q, \kappa, q_r(t)), \quad \Delta p \in \mathbf{R^n} \end{aligned} \tag{19}$$

such that

(a) the states of the closed-loop system (18), (19) are well-defined on $[0, +\infty)$ and globally bounded;
(b) there is a finite time, $T_\epsilon > 0$, such that the closed-loop system trajectories satisfy

$$\| q(t) - q_r(t) \| < \epsilon, \quad \forall t \geq T_\epsilon > 0.$$

Throughout this paper, we make the following assumptions.

Assumption 3.1. There exists an unknown constant, $M \geq 0$, such that the reference signal, $q_r(t)$, satisfies

$$\| q_r(t) \| + \| \dot{q}_r(t) \| \leq M.$$

This implies that the reference trajectories and their derivatives are bounded.

https://doi.org/10.1017/S0263574716000758 Published online by Cambridge University Press

Remark 3.1. Notice that we only assume that the reference trajectories are $\mathbf{C^1}$. This is different from SMC and many control designs which require that the reference trajectories are at least $\mathbf{C^2}$. In addition, our control law uses only the reference signal, $q_r(t)$, not its derivative. This simplifies the control design process, especially, when the required path is in a working space of a robot. In this case, one must convert the path from the working space to the joint space of the robot. This is not trivial since it involves finding the inverse Jacobian matrix and its derivative.

Assumption 3.2. $h_i(q, \dot{q}, b_{Ai}(\dot{q}_i))$ for $i = 1, \ldots, n$ does not change sign and has a lower bound, i.e. there exists an unknown, λ, such that

$$0 < \lambda \leq h_i(q, \dot{q}, b_{Ai}(\dot{q}_i)).$$

In what follows, we state some properties of the terms in Eq. (18) that will be used in the control design proof.

Property 3.1. By the definitions of b_{Di}, it is easy to see that the diagonal matrix, $B_D(\dot{q})$, is bounded by an *unknown* constant, Θ_D, such that

$$\| B_D(\dot{q}) \| \leq \Theta_D.$$

Property 3.2. A_E is a constant diagonal matrix bounded by an *unknown* constant $\Theta_E = \max\{|a_{Ei}|\} > 0$ and A_F is a constant vector bounded by an *unknown* constant $\Theta_F = \sqrt{\sum_{i=1}^{n} a_{Fi}^2} > 0$, such that

$$\| A_E \| \leq \Theta_E \quad \text{and} \quad \| A_F \| \leq \Theta_F.$$

3.2. Adaptive control design

Theorem 3.1. Under Assumptions 3.1 and 3.2, there exists a continuous adaptive controller of the form (19) that solves the problem of adaptive position tracking for all $\epsilon > 0$.

Proof. First, we define the joint position tracking error, $e \in \mathbb{R}^n$, and a filtered tracking error variable, η, as follows:

$$e = q - q_r, \tag{20}$$

$$\eta = \dot{q} + (\kappa + 1)e, \tag{21}$$

where κ is a monotone adaptive gain to be determined later. The definition (21) can also be written in terms of the joint velocity,

$$\dot{q} = \eta - (\kappa + 1)e. \tag{22}$$

Differentiating Eq. (22) with respect to time, gives

$$\ddot{q} = \dot{\eta} - \dot{\kappa}e - (\kappa + 1)\dot{q} + (\kappa + 1)\dot{q}_r. \tag{23}$$

Substituting Eqs. (22) and (23) into Eq. (18) yields the tracking error system,

$$\begin{aligned} D(q)\dot{\eta} = &-H(q, \dot{q}, b_{Ai}(\dot{q}_i))\Delta p - B_D(\dot{q})\dot{q} - A_E q - A_F + D(q)\dot{\kappa}e + D(q)(\kappa + 1)\dot{q} \\ &-D(q)(\kappa + 1)\dot{q}_r - C(q, \dot{q})\eta + C(q, \dot{q})(\kappa + 1)e - G(q) - \tau_d. \end{aligned} \tag{24}$$

Consider a Lyapunov function candidate,

$$V = \frac{1}{2\lambda}\eta^T D(q)\eta + \frac{1}{2}e^T e, \tag{25}$$

https://doi.org/10.1017/S0263574716000758 Published online by Cambridge University Press

where λ is the lower bound of $h_i(\cdot)$ in Assumption 3.2. Define the governing equation of the monotone adaptive function, κ, as

$$\dot{\kappa} = \begin{cases} \beta\{\| q - q_r \|^{\frac{1}{2}} - (\frac{\epsilon}{2})^{\frac{1}{2}}\}, & \| q - q_r \| \geq \frac{\epsilon}{2} \\ 0, & \| q - q_r \| < \frac{\epsilon}{2} \end{cases}, \ \kappa(0) \geq 1, \tag{26}$$

where β is a positive constant. From the construction of $\dot{\kappa}$, the gain, $\kappa \geq 1$, is non-decreasing. The continuous adaptive control law is to ensure a fast convergent rate of the tracking error. Then, the time derivative of Eq. (25) along the trajectories of the system (24) satisfies

$$\begin{aligned} \dot{V} &= \frac{1}{\lambda}\eta^T D(q)\dot{\eta} + \frac{1}{2\lambda}\eta^T \dot{D}(q)\eta + e^T\dot{e} \\ &= -\frac{1}{\lambda}\eta^T H(\cdot)\Delta p + \frac{1}{\lambda}\eta^T\{-B_D(\dot{q})\dot{q} - A_E q - A_F\} \\ &\quad + \frac{1}{\lambda}\eta^T\{D(q)\dot{\kappa}e + D(q)(\kappa+1)\dot{q} - D(q)(\kappa+1)\dot{q}_r + C(q,\dot{q})(\kappa+1)e - G(q) - \tau_d\} \\ &\quad + \frac{1}{2\lambda}\eta^T\left\{\dot{D}(q) - 2C(q,\dot{q})\right\}\eta + e^T\eta - (\kappa+1)e^Te - e^T\dot{q}_r. \end{aligned} \tag{27}$$

With the help of Properties 2.1–2.4, Assumptions 2.1 and 3.1, Properties 3.1 and 3.2 and the definition of $\dot{\kappa}$ in Eq. (26), we have

$$\begin{aligned} \dot{V} \leq & -\frac{1}{\lambda}\eta^T H(\cdot)\Delta p + \frac{1}{\lambda}\|\eta\|\{\Theta_D\|\dot{q}\| + \Theta_E\|e\| + \Theta_E M + \Theta_F + \mu_M\beta\|e\|^{\frac{3}{2}} \\ & -\mu_M\beta\left(\frac{\epsilon}{2}\right)^{\frac{1}{2}}\|e\| + (\kappa+1)\mu_M\|\dot{q}\| + (\kappa+1)\mu_M M + (\kappa+1)C_M\|\dot{q}\|\|e\| + G_M \\ & + T_M\} + \|e\|\|\eta\| - (\kappa+1)e^Te + M\|e\|. \end{aligned} \tag{28}$$

Substituting Eq. (22) into Eq. (28) yields

$$\begin{aligned} \dot{V} \leq & -\frac{1}{\lambda}\eta^T H(\cdot)\Delta p + \frac{1}{\lambda}(\Theta_D + 2\mu_M)\kappa\|\eta\|^2 + \left\{\frac{1}{\lambda}(2\Theta_D + \Theta_E + 4\mu_M) + 1\right\}\kappa^2\|\eta\|\|e\| \\ & + \frac{\mu_M\beta}{\lambda}\|\eta\|\|e\|^{\frac{3}{2}} + \frac{2C_M}{\lambda}\kappa\|\eta\|^2\|e\| + \frac{4C_M}{\lambda}\kappa^2\|\eta\|\|e\|^2 \\ & + \frac{1}{\lambda}(\Theta_E M + \Theta_F + 2\mu_M M + G_M + T_M)\|\eta\| - (\kappa+1)e^Te + M\|e\|. \end{aligned} \tag{29}$$

By using the completion of square, it can be shown that

$$\dot{V} \leq -\frac{1}{\lambda}\eta^T H(\cdot)\Delta p + \|\eta\|^2\Psi(\cdot) - e^Te + \frac{\Theta}{\kappa}, \tag{30}$$

where
$\Psi(\cdot) = \kappa^3\left(\|\eta\|^2 + \|\eta\|^2\|e\|^2\right) + \kappa^5\left(\|e\|^2 + \|e\|^4\right) + \kappa^3 + \kappa\|e\|^3$ and the unknown constant,
$\Theta = (\frac{\Theta_D+2\mu_M}{\lambda})^2 + (\frac{2\Theta_D+\Theta_E+4\mu_M}{\lambda} + 1)^2 + (\frac{\mu_M\beta}{\lambda})^2 + (\frac{2C_M}{\lambda})^2 + (\frac{4C_M}{\lambda})^2 + (\frac{\Theta_E M+\Theta_F+2\mu_M M+G_M+T_M}{\lambda})^2 + M^2$, is independent of κ.

From Assumption 3.2, we have $\forall h_i(\cdot) > 0$. Thus, the matrix, $H(\cdot) = diag\{h_1(\cdot), ..., h_n(\cdot)\}$, is symmetric positive definite satisfying

$$\eta^T H(\cdot)\eta \geq 0. \tag{31}$$

Select the controller for each joint as

$$\Delta p_i = \eta_i\left(\Psi(\cdot) + 1\right). \tag{32}$$

https://doi.org/10.1017/S0263574716000758 Published online by Cambridge University Press

Then, the control input vector, Δp, can be written as

$$\Delta p = (\Psi(\cdot) + 1)\,\eta.$$

Also, observe that

$$\eta^T H(\cdot)\,(\Psi(\cdot) + 1)\,\eta \geq 0 \quad \text{or} \quad \eta^T H(\cdot)\Delta p \geq 0.$$

Then, it can be shown that

$$-\frac{1}{\lambda}\eta^T H(\cdot)\Delta p = -\frac{1}{\lambda}\eta^T H(\cdot)\,(\Psi(\cdot) + 1)\,\eta = -\sum_{i=1}^{n} \eta_i^2 \frac{h_i(\cdot)}{\lambda}\,(\Psi(\cdot) + 1)$$
$$\leq -\,(\Psi(\cdot) + 1)\,\eta^T \eta. \tag{33}$$

Substituting Eq. (33) into Eq. (30) yields

$$\dot{V} \leq -\eta^T \eta - e^T e + \frac{\Theta}{\kappa} \leq -bV + \frac{\Theta}{\kappa}, \tag{34}$$

where $b = \min\{1, \lambda/\mu_M\} > 0$.

In the remaining part of the proof, we show that all states of the closed-loop system (24), (32) and (26) are bounded and well-defined on $[0, +\infty)$. Given any $\epsilon > 0$, there exists a finite time T_ϵ such that the position tracking error $\|q - q_r\| \leq \epsilon, \forall t \geq T_\epsilon$.

Since the monotone gain, $\kappa(t) \geq 1$, we obtain

$$\dot{V} \leq -bV + \Theta, \tag{35}$$

which implies that (e, η, κ) is well-defined on $[0, +\infty)$ and (e, η) is bounded.

The compact set, $\Omega = \left\{e, \eta | V(e, \eta) \leq a, \forall a \geq \frac{\Theta}{b}\right\}$, is invariant, since V is positive definite and proper and $\dot{V}$ is negative semi-definite, $\forall e, \eta \in \Omega$. To show that $\kappa(t)$ is bounded, we use a contradiction argument. Suppose that the monotone non-decreasing function, $\kappa(t)$, is unbounded. Then, there must exist a finite time, T^*, such that

$$\kappa(t) \geq \frac{\Theta}{\epsilon^*}, \quad \epsilon^* = \frac{b\epsilon^2}{16}, \quad \forall t \geq T^*$$

and Eq. (34) becomes

$$\dot{V} \leq -bV + \epsilon^*, \quad \forall t \geq T^*.$$

Consequently,

$$V(t) \leq e^{-b(t-T^*)}\left(V(T^*) - \frac{\epsilon^*}{b}\right) + \frac{\epsilon^*}{b}, \quad \forall t \geq T^*.$$

This implies that there exists another finite time, T_1, such that

$$\frac{\|q - q_r\|^2}{2} = \frac{1}{2}\sum_{i=1}^{n} \leq V(t) < \frac{2\epsilon^*}{b} = \frac{\epsilon^2}{8}, \quad \forall t \geq T_1$$

which implies that $\dot{\kappa}(t) = 0, \forall t \geq T_1$ and leads to the contradiction of the assumption that $\kappa(t)$ is unbounded. Hence, we can conclude that all states of Eqs. (24), (32) and (26) are also bounded and well-defined on $[0, +\infty)$. From Assumption 3.1, the closed-loop system trajectories generated by Eqs. (24), (32) and (26) are well-defined and bounded on $[0, +\infty)$.

https://doi.org/10.1017/S0263574716000758 Published online by Cambridge University Press

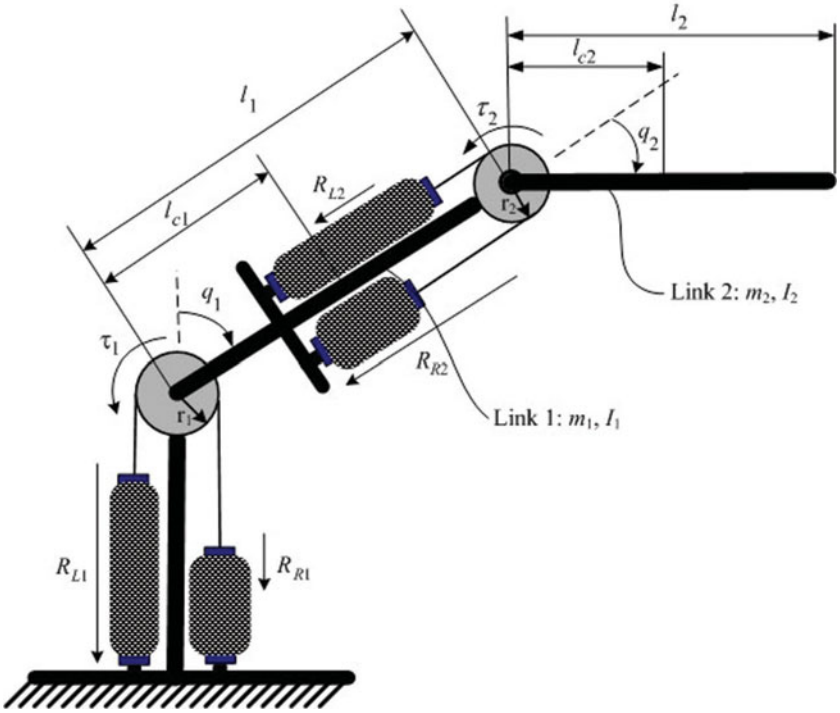


Fig. 4. The two-link robot arm actuated by pneumatic muscles.

In addition, the integral of $\dot{\kappa}(t)$ evaluated from zero to infinity exists and is finite, i.e.

$$\lim_{t\to+\infty}\int_0^t \dot{\kappa}d\tau = \kappa(\infty) - \kappa(0).$$

Then, it follows from *Barbalat 's lemma* that

$$\lim_{t\to+\infty}\dot{\kappa}(t) = 0.$$

This, together with Eq. (26), implies the existence of a finite time, T_ϵ, satisfying

$$\|q(t) - q_r(t)\| \le \epsilon, \quad t \ge T_\epsilon > 0.$$

□

4. Simulation Results

In order to demonstrate the performance of the proposed adaptive control scheme, we consider applying the control scheme to a two-link robot arm actuated by pneumatic muscles as shown in Fig. 4.

The revolute joint 1 and 2 are rotatable through the angles $-\pi < q_1, q_2 < \pi$ rad. The dynamics of the two-link robot arm actuated by pneumatic muscles with joint frictions can be described as

$$\begin{bmatrix} d_{11} & d_{12} \\ d_{21} & d_{22} \end{bmatrix}\begin{bmatrix} \ddot{q}_1 \\ \ddot{q}_2 \end{bmatrix} = -\begin{bmatrix} h_1(\cdot) & 0 \\ 0 & h_2(\cdot) \end{bmatrix}\begin{bmatrix} \Delta p_1 \\ \Delta p_2 \end{bmatrix} - \begin{bmatrix} b_{D1}(\dot{q}_1) & 0 \\ 0 & b_{D2}(\dot{q}_2) \end{bmatrix}\begin{bmatrix} \dot{q}_1 \\ \dot{q}_2 \end{bmatrix}$$
$$- \begin{bmatrix} a_{E1} & 0 \\ 0 & a_{E2} \end{bmatrix}\begin{bmatrix} q_1 \\ q_2 \end{bmatrix} - \begin{bmatrix} a_{F1} \\ a_{F2} \end{bmatrix} - \begin{bmatrix} c_{11} & c_{12} \\ c_{21} & c_{22} \end{bmatrix}\begin{bmatrix} \dot{q}_1 \\ \dot{q}_2 \end{bmatrix} - \begin{bmatrix} g_1 \\ g_2 \end{bmatrix} - \begin{bmatrix} \tau_{d1} \\ \tau_{d2} \end{bmatrix},$$

https://doi.org/10.1017/S0263574716000758 Published online by Cambridge University Press

where

$$h_1(\cdot) = b_{A1}(t)\dot{q}_1 + a_{B1}q_1 + a_{C1}, \qquad h_2(\cdot) = b_{A2}(t)\dot{q}_2 + a_{B2}q_2 + a_{C2},$$

$$b_{A1}(\dot{q}_1) = \begin{cases} -n_1(B_{1L1i} + B_{1R1d})r_1^2, & \dot{q}_1 < 0 \\ 0, & \dot{q}_1 = 0, \\ n_1(B_{1L1d} + B_{1R1i})r_1^2, & \dot{q}_1 > 0 \end{cases} \quad b_{A2}(\dot{q}_2) = \begin{cases} -n_2(B_{1L2i} + B_{1R2d})r_2^2, & \dot{q}_2 < 0 \\ 0, & \dot{q}_2 = 0, \\ n_2(B_{1L2d} + B_{1R2i})r_2^2, & \dot{q}_2 < 0 \end{cases}$$

$$a_{B1} = n_1(K_{1R1} - K_{1L1})r_1^2 a_{B2} = n_2(K_{1R2} - K_{1L2})r_2^2,$$

$$a_{C1} = n_1(2F_{2R1}P_{0R1} - F_{1R1} + 2F_{2L1}P_{0L1} - F_{1L1} + r_1K_{1R1}\pi + r_1K_{1L1}\pi)r_1,$$

$$a_{C2} = n_2(2F_{2R2}P_{0R2} - F_{1R2} + 2F_{2L2}P_{0L2} - F_{1L2} + r_2K_{1R2}\pi + r_2K_{1L2}\pi)r_2,$$

$$b_{D1}(\dot{q}_1) = \begin{cases} -n_1(B_{0L1i} + B_{1L1i}P_{0L1} \\ +B_{0R1d} - B_{1R1d}P_{0R1})r_1^2, & \dot{q}_1 < 0 \\ 0, & \dot{q}_1 = 0, \\ -n_1(B_{0L1d} - B_{1L1d}P_{0L1} \\ +B_{0R1i} + B_{1R1i}P_{0R1})r_1^2, & \dot{q}_1 > 0 \end{cases} \quad b_{D2}(\dot{q}_2) = \begin{cases} -n_2(B_{0L2i} + B_{1L2i}P_{0L2} \\ +B_{0R2d} - B_{1R2d}P_{0R2})r_2^2, & \dot{q}_2 < 0 \\ 0, & \dot{q}_2 = 0, \\ -n_2(B_{0L2d} - B_{1L2d}P_{0L2} \\ +B_{0R2i} + B_{1R2i}P_{0R2})r_2^2, & \dot{q}_2 > 0 \end{cases}$$

$$a_{E1} = -n_1(K_{1L1}P_{0L1} + K_{1R1}P_{0R1} + K_{0L1} + K_{0R1})r_1^2,$$

$$a_{E2} = -n_2(K_{1L2}P_{0L2} + K_{1R2}P_{0R2} + K_{0L2} + K_{0R2})r_2^2,$$

$$\begin{aligned} a_{F1} = -n_1(&F_{2R1}P_{0R1}^2 - F_{1R1}P_{0R1} - F_{2L1}P_{0L1}^2 + F_{1L1}P_{0L1} + r_1K_{1R1}P_{0R1}\pi + r_1K_{0R1}\pi \\ &-r_1K_{1L1}P_{0L1}\pi - r_1K_{0L1}\pi)r_1, \end{aligned}$$

$$\begin{aligned} a_{F2} = -n_2(&F_{2R2}P_{0R2}^2 - F_{1R2}P_{0R2} - F_{2L2}P_{0L2}^2 + F_{1L2}P_{0L2} + r_2K_{1R2}P_{0R2}\pi + r_2K_{0R2}\pi \\ &-r_2K_{1L2}P_{0L2}\pi - r_2K_{0L2}\pi)r_2, \end{aligned}$$

$$d_{11} = m_2(2l_1l_{c2}\cos q_2 + l_{c2}^2 + l_1^2) + m_1l_{c1}^2 + I_1 + I_2,$$

$$d_{12} = m_2(l_{c2}^2 + l_1l_{c2}\cos q_2)) + I_2, \quad d_{21} = d_{12}, \quad d_{22} = m_2l_{c2}^2 + I_2,$$

$$c_{11} = -m_2l_1l_{c2}\dot{q}_2\sin q_2 \quad c_{12} = -m_2l_1l_{c2}(\dot{q}_1 + \dot{q}_2)\sin q_2,$$

$$c_{21} = m_2l_1l_{c2}\dot{q}_1\sin q_2, \quad c_{22} = 0,$$

$$g_1 = -m_1gl_{c1}\sin q_1 - m_2g(l_1\sin q_1 + l_{c2}\sin(q_1 + q_2)), \quad g_2 = -m_2gl_{c2}\sin(q_1 + q_2),$$

where $m_1, m_2, l_1, l_2, l_{c1}, l_{c2}, r_1, r_2, I_1$ and I_2 denote the masses, link lengths, sprocket radius and the inertias of the each link, respectively and g is the Earth gravity.

The closed-loop system is simulated with the following physical parameters, $l_1 = l_2 = 0.5$ m, $l_{c1} = l_{c2} = 0.25$ m, $m_1 = 7.5$ kg, $m_2 = 7$ kg, $r_1 = 0.07$ m, $r_2 = 0.06$ m and the numbers of the muscle pairs $n_1 = 6$ and $n_2 = 3$. All of the simulations are performed with the initial conditions, $q_1(0) = 0.6$ rad., $q_2(0) = 1.0$ rad., $\dot{q}_1(0) = \dot{q}_2(0) = 0$ rad./s, $\epsilon = 0.1$ rad., $\beta = 80$, the nominal pressures $P_{0R1} = P_{0R2} = 420$ kPa and $P_{0L1} = P_{0L2} = 405$ kPa and the joint frictions, $\tau_d = [2\text{sgn}(\dot{q}_1) \quad 2\text{sgn}(\dot{q}_2)]^T$.

In the simulations, we study five cases of muscle parameter sets as shown in Table 1. The nominal values of the muscle parameters are obtained from those in Reynolds *et al.*[10] Case A represents the system under normal condition and has a matching pair of muscle groups. Case B through E represent the systems with mismatched pairs of muscle groups or undergoing severe changes of muscle properties. In all cases, all parameters of each muscle pairs are changed by the same absolute percentage as shown in Table 1. The internal pressure in each muscle are restricted within the range, $206.844 \leq P \leq 620.532$ kPa since the parameters of the muscles are only applicable in this pressure range.

https://doi.org/10.1017/S0263574716000758 Published online by Cambridge University Press

Table I. Case studies for investigate tracking performance.

Case	Right1 (R1)	Left1 (L1)	Right2 (R2)	Left2 (L2)
A	Nominal	Nominal	Nominal	Nominal
B	minus 30%	plus 30%	minus 30%	plus 30%
C	plus 30%	minus 30%	plus 30%	minus 30%
D	minus 30%	plus 30%	plus 30%	minus 30%
E	plus 30%	minus 30%	minus 30%	plus 30%

The controller performance is investigated by making the end effector follow a hexagonal shape in x–y work space. The parametric equations of a hexagonal are shown below:

$$x_d = \begin{cases} 0.5112 - 0.1212\cos(0.8\pi\bar{t}), & 0 < \bar{t} \le 1.25 \\ 0.5112 - 0.1212\cos(0.8\pi\bar{t}), & 1.25 < \bar{t} \le 2.5 \\ 0.25 + 0.14\cos(0.8\pi\bar{t}), & 2.5 < \bar{t} \le 3.75 \\ -0.5112 - 0.1212\cos(0.8\pi\bar{t}), & 3.75 < \bar{t} \le 5 \\ -0.5112 - 0.1212\cos(0.8\pi\bar{t}), & 5 < \bar{t} \le 6.25 \\ 0.25 + 0.14\cos(0.8\pi\bar{t}), & 6.25 < \bar{t} \le 7.5 \end{cases}, \tag{36}$$

$$y_d = \begin{cases} 0.2288 - 0.1212\cos(0.8\pi\bar{t}), & 0 < \bar{t} \le 1.25 \\ 0.4712 + 0.1212\cos(0.8\pi\bar{t}), & 1.25 < \bar{t} \le 2.5 \\ 0.5925, & 2.5 < \bar{t} \le 3.75 \\ 0.4712 - 0.1212\cos(0.8\pi\bar{t}), & 3.75 < \bar{t} \le 5 \\ 0.2288 + 0.1212\cos(0.8\pi\bar{t}), & 5 < \bar{t} \le 6.25 \\ 0.1075, & 6.25 < \bar{t} \le 7.5 \end{cases}, \tag{37}$$

where $\bar{t} = rem(t, 7.5)$, and x_d and y_d are the desired end-effector spatial trajectories along x and y axes. The inverse kinematics of the planar arm in Fig. 3 can be computed by

$$q_{2r} = \arccos\left(\frac{x_d^2 + y_d^2 - l_1^2 - l_2^2}{2l_1 l_2}\right),$$
$$q_{1r} = \arctan\left(\frac{x_d}{y_d}\right) - \arctan\left\{\frac{l_2 \sin q_2}{l_1 + l_2 \cos q_2}\right\}.$$

Notice that Eqs. (36) and (37) are only $\mathbf{C^1}$. The SMC,[11, 12] BASMC,[14-17] PBSMC,[19, 20] and CRVC[21, 22] require $\mathbf{C^2}$ reference signals. Therefore, these trajectories are not applicable for these control schemes. In addition, the proposed control law only uses the joint trajectories, not their derivatives. Compared to other control laws that require the joint derivatives, $\mathbf{C^2}$ reference signals in joint space can be obtained via the differential kinematics and its time derivative. They exist only when the robot does not move into a singular configuration, i.e. the Jacobian matrix remains non-singular. Our controller is continuous, thus there is no chattering and the adaptive gain is only increased to the level that ensures the errors are within the prescribed limit.

All simulations have performed for 1000 s. The simulation results of the five cases are shown in Figs. 5–11. The joint angle errors are shown in Fig. 6 while Fig. 7 shows the position error of the end effector. The tracking errors would eventually be within the prescribed error bound, $\epsilon = 0.1$ rad., roughly after 1 s in all cases. The position accuracy of the closed-loop system can be adjusted simply by changing the threshold value, ϵ, in Eq. (26) without any change in the control law. Naturally, the more accurate tracking performance, the higher gain (higher capacity of the actuator) is required. This is very convenient since the trade-off between system performance and actuator capacity can be tuned very easily. While the tracking error will be within the prescribed error bound for any positive gain β, the speed of convergence to the error bound depends on β. The higher the gain β, the faster the error will converge and also the higher capacity of the actuator is required.

The pressure inputs, Δp_1 and Δp_2, are shown in Fig. 8. The internal pressures of the left muscles, P_{L1}, and the right muscles, P_{L2}, are shown in Figs. 9. and 10, respectively. In Case A, where there is

https://doi.org/10.1017/S0263574716000758 Published online by Cambridge University Press

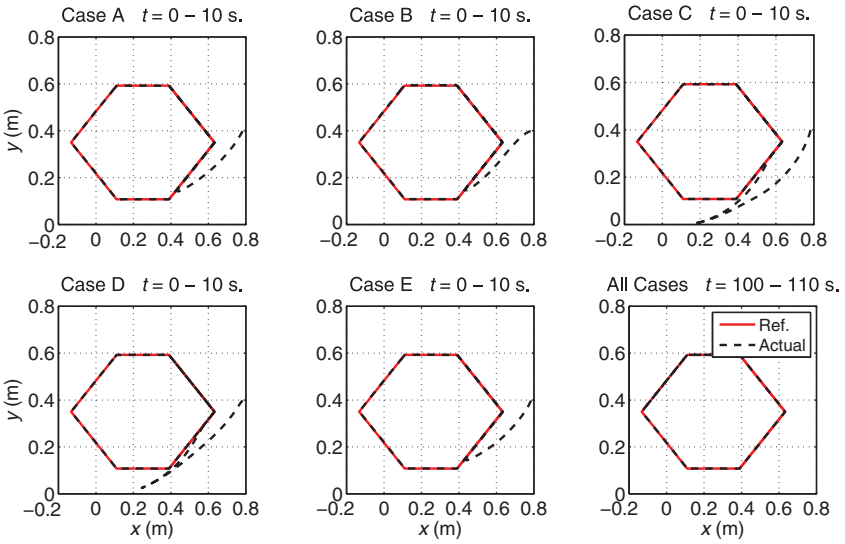


Fig. 5. End-effector spatial trajectories ($x(0) = 0.8$ m, $y(0) = 0.4$ m).

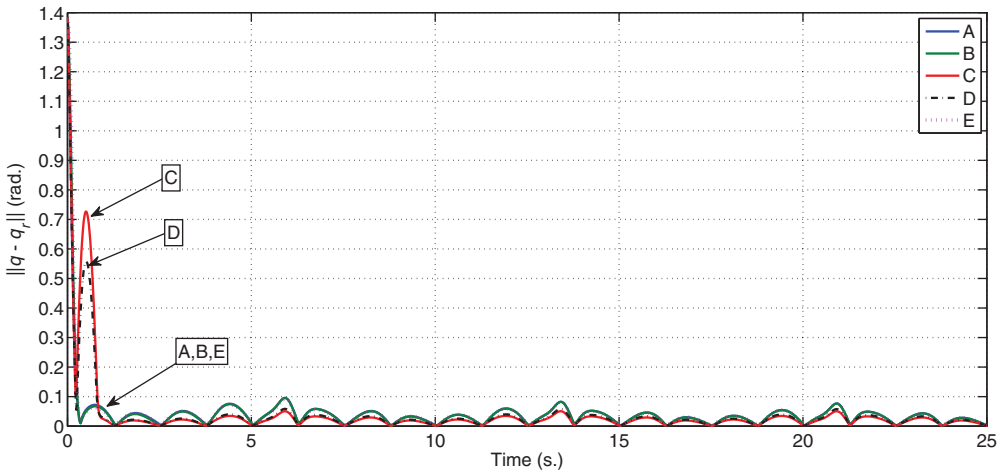


Fig. 6. Norms of the joint position errors.

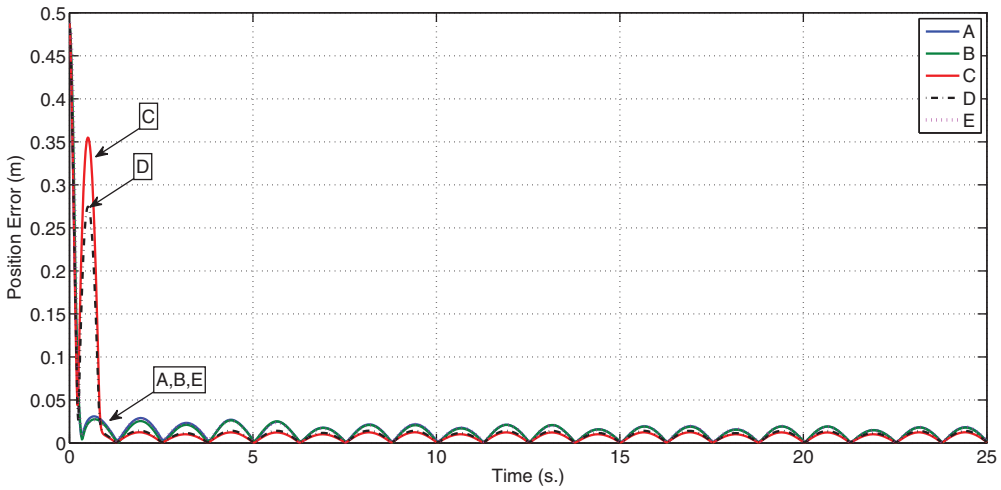


Fig. 7. Norms of the end-effector position errors.

https://doi.org/10.1017/S0263574716000758 Published online by Cambridge University Press

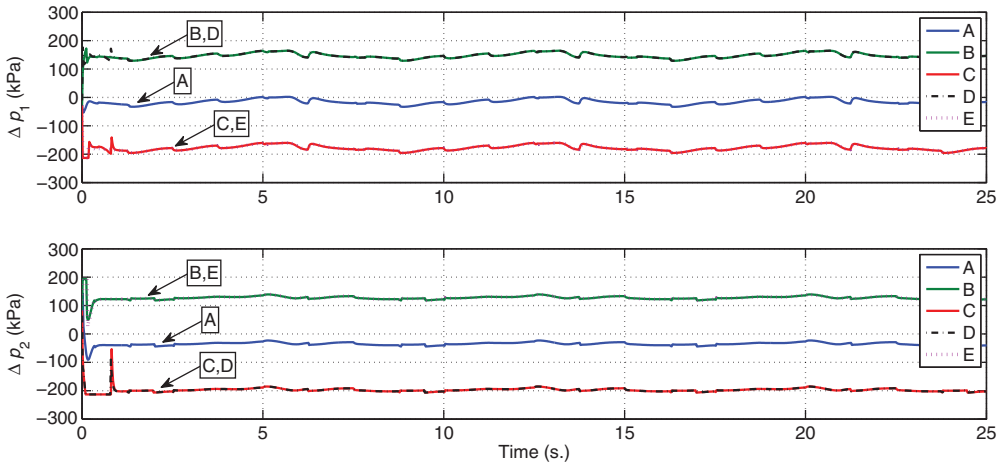


Fig. 8. Pressure inputs.

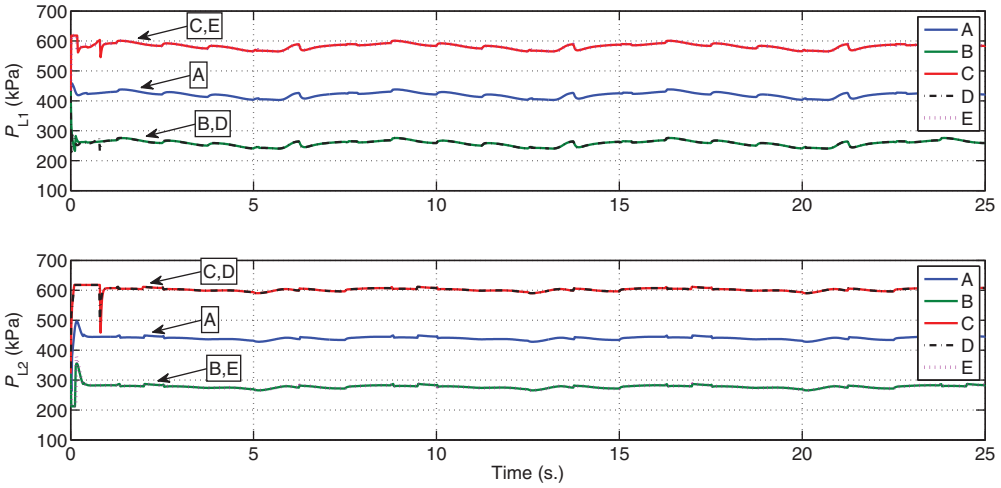


Fig. 9. Internal pressures of the left muscles.

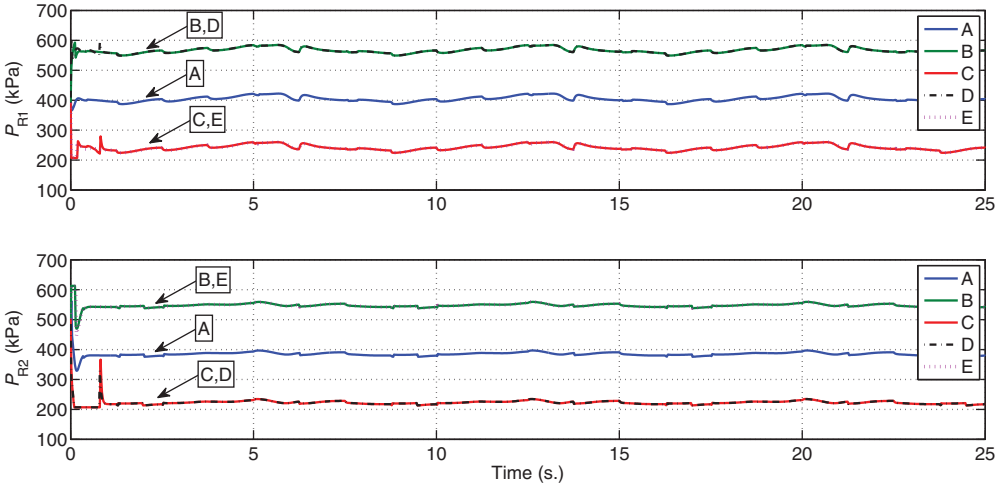


Fig. 10. Internal pressures of the right muscles.

https://doi.org/10.1017/S0263574716000758 Published online by Cambridge University Press

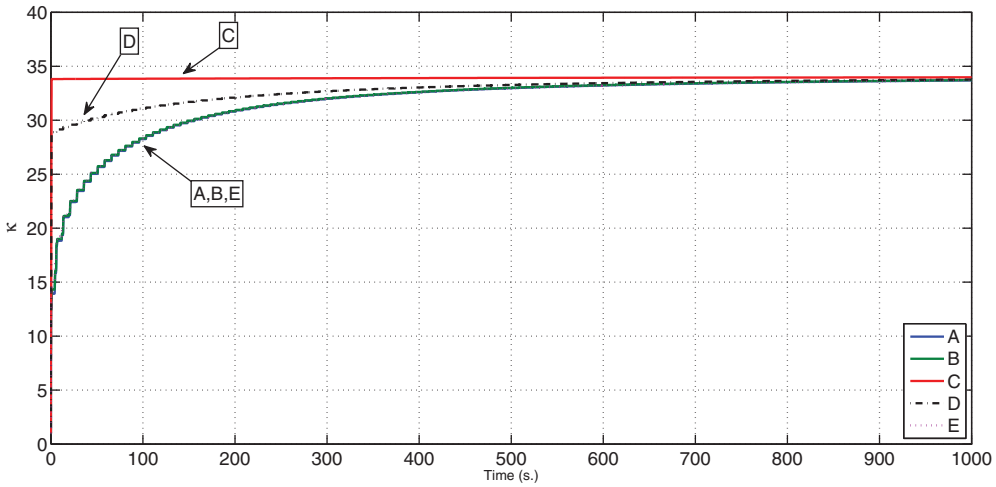


Fig. 11. Adaptive gains.

no muscle mismatch, the pressures in all muscles stay within the operational values, $206.844 \leq P \leq 620.532$ kPa. Pressure saturation does not occur. In the other cases, parameter values are purposely chosen such that the pressures in muscles can saturate. It can be seen that the controller is very robust and the closed-loop system is stable even under input saturations.

The adaptive gain is shown in Fig. 11. The simulation results show that the gains defined by Eq. (26) are really bounded and converge to almost the same value in all cases. The main difference is in the transient period where the adaptive gains in Case C and D converge to the final value faster than the gains in the other cases. This is because with these initial states, the trajectories in Case C and D deviate from the reference trajectories more than those in the other cases. This can be seen from the trajectories in Figs. 5 and 6.

In what follows, a comparison of the closed-loop performances of a SMC and the proposed controller is included. The robot model (18) can be written as

$$\ddot{q} = M(q, \dot{q})\Delta p + N(q, \dot{q}), \tag{38}$$

where $M(q, \dot{q}) = -D^{-1}(q)H(\cdot)$ and $N(q, \dot{q}) = D^{-1}(q)\{-C(q, \dot{q})\dot{q} - G(q) - \tau_d - B_D(\dot{q})\dot{q} - A_E q - A_F\}$. For the system (38), an SMC can be chosen as[15–17]

$$\Delta p = \hat{M}^{-1}\{-\hat{N} - \ddot{q}_r - \lambda\dot{e} - K_s sat(\frac{\sigma}{\Gamma})\}, \tag{39}$$

where the sliding surface $\sigma = \dot{e} + \lambda e$, and $\hat{M}$ and $\hat{N}$ are the estimates of M and N, respectively. K_s is the controller gain and $sat(\cdot)$ is used to suppress chattering.

The closed-loop simulation with Eq. (39) was performed with the nominal muscle parameters (Case A), the functions $\hat{M} = M$ and $\hat{N} = N$, and the following parameters $\lambda = 5, \Gamma = 0.5$ and $K_s = 80$. The boundary layer thickness Γ is chosen so that convergence region is comparable to prescribed error of 0.1 rad. Since $\hat{M} = M$ and $\hat{N} = N$, this represents an ideal case for the SMC (39) in which all of the system parameters are precisely known and all of non-linearities can be canceled. However, the term $\ddot{q}_r$ does not exist and is not available for feedback since Eqs. (36) and (37) are only $\mathbf{C^1}$.

Figures 12 and 13 show that SMC cannot regulate the error to be within the prescribed error bound. The error is highest at corners where the second derivatives of the reference trajectories do not exist. This shows that a tracking problem of $\mathbf{C^1}$ reference trajectories cannot be trivially solved by SMC even under the case that perfect knowledge of the system is assumed.

https://doi.org/10.1017/S0263574716000758 Published online by Cambridge University Press

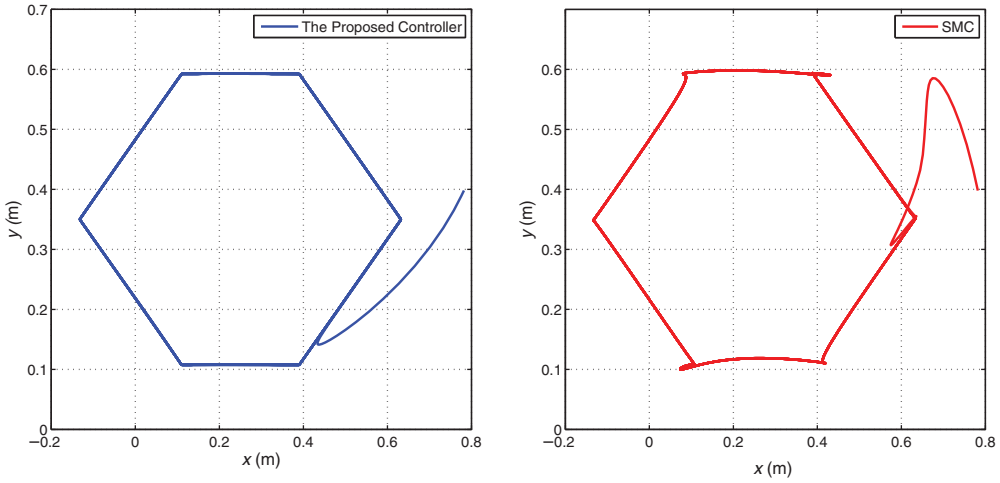


Fig. 12. End-effector spatial trajectories of the proposed controller and SMC.

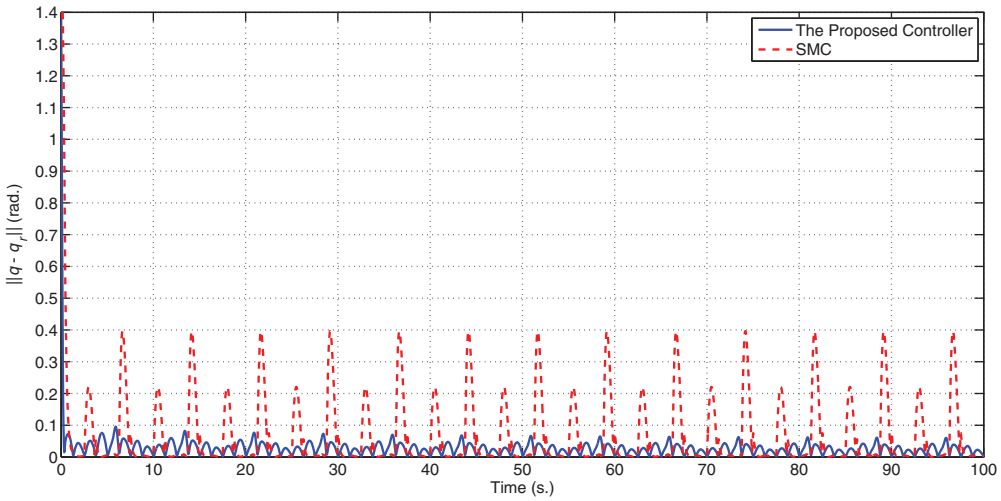


Fig. 13. Norms of the joint position errors of the proposed controller and SMC.

5. Conclusions

In this paper, an adaptive tracking control scheme was developed for a multi-link robot actuated by pneumatic muscles with time-varying additive disturbances under the conditions that all physical parameters of the muscle and robot are unknown and not constant. This parameter-free control law provides a universal controller for a multi-link robot actuated by pneumatic muscles in the sense that one controller can be used with any rigid link robot actuated by pneumatic muscles without any modification. The proposed control law can follow any $\mathbf{C}^1$ trajectory. The closed-loop states are globally bounded and the joint position errors will be within a prescribed error bound in a finite time. The new continuous adaptive gain can provide fast convergent speed of the error. The performance and characteristic are demonstrated by simulations. The simulations show that the adaptive control scheme can achieve joint position tracking even under severe changes of system parameters and discontinuous additive disturbances.

Acknowledgments

This work was supported by CMU Short Term Research Fellowships in Overseas. The authors also thank Ms Wiriya Sungkhaniyom and Dr Matthew Cole for their proofreading help.

https://doi.org/10.1017/S0263574716000758 Published online by Cambridge University Press

References

1. F. Daerden and D. Lefeber, "The concept and design of pleated pneumatic artificial muscles," *Int. J. Fluid Power* **2**(3), 41–50 (2001).
2. J. M. Yarlott, "Fluid actuator," U.S. Patent 3 645 173, Feb. 29, (1972).
3. G. Immega and M. Kukolj, "Axially contractable actuator," U.S. Patent 4 939 982, (Jul. 10, 1990).
4. H. M. Paynter, "Hyperboloid of revolution fluid-driven tension actuators and methods of making," U.S. Patent 4 721 030, (Jan. 26, 1988).
5. G. Andrikopoulos, G. Nikolakopoulos and S. Manesis, "A Survey on Applications of Pneumatic Artificial Muscles," *Proceedings of the MED Conf. Control Autom.*, Corfu, Greece (Jun. 2011) pp. 1439–1446.
6. C. P. Chou and B. Hannaford, "Static and Dynamic Characteristics of McKibben Pneumatic Artificial Muscles," *Proceedings of the IEEE International Conference on Robotics and Automation*, San Diego, CA, USA (May 1994) pp. 281–286.
7. C. P. Chou and B. Hannaford, "Measurement and modeling of McKibben pneumatic artificial muscles," *IEEE Trans. Robot. Autom.* **12**(1), 90–102 (Feb. 1996).
8. B. Tondu and P. Lopez, "Modeling and control of McKibben pneumatic artificial muscle robot actuators," *IEEE Control Syst.* **20**(2), 15–38 (Apr. 2000).
9. D. W. Repperger, K. R. Johnson and C. A. Phillips, "Nonlinear Feedback Controller Design of a Pneumatic Muscle Actuator System," *Proceedings of the Amer. Control Conf.*, San Diego, CA (Jun. 1999) pp. 1525–1529.
10. D. B. Reynolds, D. W. Repperger, C. A. Phillips and G. Bandry, "Modeling the dynamic characteristics of pneumatic muscle," *Ann. Biomed. Eng.* **31**(3), 310–317 (Mar. 2003).
11. D. W. Cai and H. Yamaura, "A Robust Controller for Manipulator Driven by Artificial Muscle Actuator," *Proceedings of the IEEE International Conference on Control Applications*, Dearborn, MI (Sep. 1996) pp. 540–545.
12. D. W. Cai and Y. Dai, "A Sliding Mode Controller for Manipulator Driven by Artificial Muscle Actuator," *Proceedings of IEEE International Conference on Control Applications*, Anchorage, AK (Sep. 2000) pp. 668–673.
13. L. Zhang, J. Xie and D. Lu, "Adaptive robust control of one-link joint actuated by pneumatic artificial muscles," *Proceedings of IEEE/ICBBE International Conference on Bioinformatics and Biomedical Engineering*, Wuhan, Hubei, China (Jul. 2007) pp. 1185–1189.
14. J. H. Lilly and P. M. Quesada, "A two-input sliding-mode controller for a planar arm actuated by four pneumatic muscle groups," *IEEE Trans. Neural Syst. Rehabil. Eng.* **12**(3), 349–359 (Sep. 2004).
15. J. H. Lilly and L. Yang, "Sliding mode tracking for pneumatic muscle actuators in opposing pair configuration," *IEEE Trans. Control Syst. Technol.* **13**(4), 550–558 (Jul. 2005).
16. K. Xing, J. Huang, Y. Wang, J. Wu, Q. Xu and J. He, "Tracking control of pneumatic artificial muscle actuators based on sliding mode and non-linear disturbance observer," *IET Control Theory Appl.* **4**(10), 2058–2070 (Oct. 2010).
17. T. Y. Choi, B. S. Choi and K. H. Seo, "Position and compliance control of a pneumatic muscle actuated manipulator for enhanced safety," *IEEE Trans. Control Syst. Technol.* **19**(4), 832–842 (Jul. 2011).
18. H. Aschemann and D. Schindele, "Sliding-mode control of a high-speed linear axis driven by pneumatic muscle actuators," *IEEE Trans. Ind. Electron.* **55**(11), 3855–3864 (Nov. 2008).
19. M. Van Damme, B. Vanderborght, B. Verrelst, R. Van Ham, F. Daerden and D. Lefeber, "Proxy-based sliding mode control of a planar pneumatic manipulator," *Int. J. Robot. Res.* **28**(2), 266–284 (Feb. 2009).
20. P. Beyl, M. Van Damme, R. Van Ham, R. Versluys, B. Vanderborght and D. Lefeber, "An Exoskeleton for Gait Rehabilitation: Prototype Design and Control Principle," *Proceedings of the 2008 IEEE International Conference on Robotics and Automation*, Pasadena, CA (May 2008) pp. 2037–2042.
21. T. Y. Choi and J. J. Lee, "Control of manipulator using pneumatic muscles for enhanced safety," *IEEE Trans. Ind. Electron.* **57**(8), 2815–2825 (Aug. 2010).
22. S. Hussain, S. Q. Xie and P. K. Jamwal, "Robust nonlinear control of an intrinsically compliant robotic gait training orthosis," *IEEE Trans. Syst. Man Cybern. A* **43**(3), 655–665 (May 2013).
23. J. Wu, T. wang and K. Xing, "Nonlinear disturbance observer-based dynamic surface control for trajectory tracking of pneumatic muscle system," *IEEE Trans. Control Syst. Technol.* **22**(2), 440–455 (Mar. 2014).
24. J. H. Lilly, "Adaptive tracking for pneumatic muscle actuators in bicep and tricep configurations," *IEEE Trans. Neural Syst. Rehabil. Eng.* **11**(3), 333–339 (Sep. 2003).
25. G. Tonietti and A. Bicchi, "Adaptive Simultaneous Position and Stiffness Control for a Soft Robot Arm," *Proceedings of the IEEE/RSJ Conference on Intelligent Robots and Systems*, Lausanne, Switzerland, vol. 2, (Oct. 2002) pp. 1992–1997.
26. Y. Xu, "Chattering free robust control for nonlinear systems," *IEEE Trans. Control Syst. Technol.* **16**(6), 1352–1359 (Nov. 2008).
27. R. Potluri, "Comments on 'chattering free robust control for nonlinear systems'," *IEEE Trans. Control Syst. Technol.* **20**(2), 562 (Mar. 2012).
28. Y. Xu and N. Li, "Authors' reply to "comments on 'chattering free robust control for nonlinear systems"'," *IEEE Trans. Control Syst. Technol.* **20**(2), 563 (Mar. 2012).
29. C. H. Xiong, X. Z. Jiang, R. L. Sun, X. L. Huang and Y. L. Xiong, "Control methods for exoskeleton rehabilitation robot driven with pneumatic muscles," *Ind. Robot: An Int. J.* **36**(3), 210–220 (2009).

https://doi.org/10.1017/S0263574716000758 Published online by Cambridge University Press

30. K. Kawashima, T. Sasaki, A. Ohkubo, T. Miyata and T. Kagawa, "Application of robot arm using fiber knitted type pneumatic artificial rubber muscles," *Proceedings of the IEEE Conf. Robot. Autom.*, New Orleans, LA, USA (Apr.-May 2004) pp. 4937–4942.
31. M.-K. Chang, "An adaptive self-organizing fuzzy sliding mode controller for a 2-DOF rehabilitation robot actuated by pneumatic muscle actuators," *Control Eng. Practice* **18**(1), 13–22 (Jan. 2010).
32. H. Jahanabadi, M. Mailah, M. Z. Md Zain and H. M. Hooi, "Active force with fuzzy logic control of a two-link arm driven by pneumatic artificial muscles," *J. Bionic Eng.* **8**(4), 474–484 (Dec. 2011).
33. TU D. C. Thanh and K. K. Ahn, "Nonlinear PID control to improve the control performance of 2 axes pneumatic artificial muscle manipulator using neural network," *Mechatronics* **16**(9), 577–587 (Nov. 2006).
34. K. K. Ahn and H. P. H. Anh, "Comparative study of modeling and identification of the pneumatic artificial muscle (PAM) manipulator using recurrent neural networks," *J. Mech. Sci. Technol.* **22**(7), 1287–1298 (Jul. 2008).
35. D. Schindele and H. Aschemann, "ILC for a Fast Linear Axis Driven by Pneumatic Muscle Actuators," *Proceedings of IEEE International Conference on Mechatronics (ICM)*, Istanbul, Turkey (Apr. 2011) pp. 967–972.
36. D. Schindele and H. Aschemann, "P-type ILC with Phase Lead Compensation for a Pneumatically Driven Parallel Robot," *Proceedings of the American Control Conference 2012 (ACC)*, Montreal, Canada (Jun. 2012) pp. 5484–5489.
37. T. Karnjanaparichat and R. Pongvuthithum, "Adaptive control for a one-link robot arm actuated by pneumatic muscles," *Chiang Mai J. Sci.* **35**(3), pp. 437–446 (Sep. 2008).

https://doi.org/10.1017/S0263574716000758 Published online by Cambridge University Press